physica status solidi b

phys. stat. sol. (b) **243**, No. 14, 3682–3691 (2006) / **DOI** 10.1002/pssb.200642228

Feature Article

Control and measurement of electron spins in semiconductor quantum dots

L. P. Kouwenhoven, J. M. Elzerman*, R. Hanson, L. H. Willems van Beveren, and **L. M. K. Vandersypen**

Kavli Institute of Nanoscience Delft and ERATO Mesoscopic Correlation Project, Delft University of Technology, P.O. Box 5046, 2600 GA Delft, Netherlands

Received 30 April 2006, revised 19 July 2006, accepted 7 August 2006
Published online 8 November 2006

PACS 03.67.Lx, 73.63.Kv, 76.30.–v

We present an overview of experimental steps taken towards using the spin of a single electron trapped in a semiconductor quantum dot as a spin qubit [Loss and DiVincenzo, Phys. Rev. A **57**, 120 (1998)]. Fabrication and characterization of a double quantum dot containing two coupled spins has been achieved, as well as initialization and single-shot read-out of the spin state. The relaxation time T_1 of single-spin and two-spin states was found to be on the order of a millisecond, dominated by spin–orbit interactions. The time-averaged dephasing time T_2^*, due to fluctuations in the ensemble of nuclear spins in the host semiconductor, was determined to be on the order of several tens of nanosceconds. Coherent manipulation of single-spin states can be performed using a microfabricated wire located close to the quantum dot, while two-spin interactions rely on controlling the tunnel barrier connecting the respective quantum dots [Petta et al., Science **309**, 2180 (2005)].

1 Introduction

In recent years, much progress has been made in measuring and controlling electron spin states in semiconductor quantum dots. It is now possible to confine a single spin in a lateral quantum dot [2] and to couple two spins in a double quantum dot [3]. We can perform single-shot measurements to read out the spin state of one electron [4] or two electrons [5] in a dot. In double dots, the Pauli spin blockade phenomenon [6] has enabled investigation of the hyperfine interaction between an electron spin and the nuclear spins of the host material [7, 8]. Understanding of these hyperfine effects in combination with pulsed control of the exchange interaction between two electrons has lead to coherent manipulation of the state of two coupled spins in separate dots [9]. Finally, very recently coherent single-spin rotations have been demonstrated [10]. We present an overview of some of these rapid developments, inspired by the goal of using single electron spins as quantum bits [1].

2 Qubit

Any implementation of a quantum bit has to satisfy the five DiVincenzo requirements [11]. The first requirement is to have a scalable physical system with well-characterized qubits. We have fabricated double quantum dot devices (Fig. 1) in which a single electron can be confined in each of the two dots [3].

* Corresponding author: e-mail: elzerman@phys.ethz.ch

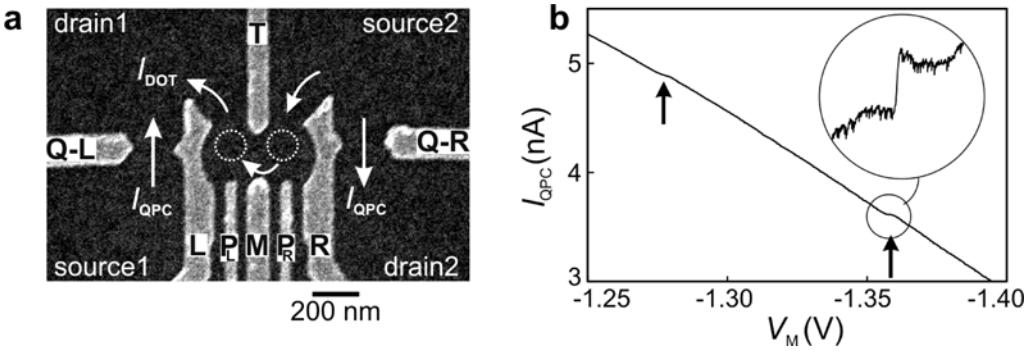

Fig. 1 Double quantum dot with two quantum point contacts (QPCs) serving as charge detectors. (a) Scanning Electron Micrograph of the metallic surface gates. White dotted circles indicate the two quantum dots, white arrows show the possible current paths. A bias voltage applied between source 2 and drain 1 leads to current through the dots, I_{DOT}. A bias voltage between source 1 (source 2) and drain 1 (drain 2), yields a current, I_{QPC}, through the left (right) QPC. (b) QPC as a charge detector of the left single dot. Plotted is the current through the left QPC versus left-dot gate voltage, V_M, with a bias voltage over the QPC of 250 μV. The steps, indicated by the arrows, correspond to a change in the electron number of the left dot. Encircled inset: the last step (50 pA high), with the linear background subtracted.

The spin states ↑ and ↓ of the electron, subject to a large magnetic field B, correspond to the two states of the proposed qubit two-level system. The Zeeman splitting, ΔE_Z, between the two states can be tuned with the magnetic field, according to $\Delta E_Z = g\mu_B B$, with $g \approx -0.44$ the electronic g-factor in GaAs [12, 13] and μ_B the Bohr magneton.

These one-electron dots can be fully characterized using a QPC as a charge detector [14]. First of all, we can use the QPC to monitor the charge configuration of the double dot [3], in order to reach the regime where both dots contain just a single electron. Then we can evaluate and tune the tunnel rate from each dot to the reservoir using a lock-in technique [15]. The same technique can be employed to determine the energy spectrum of each of the two dots, i.e. the Zeeman splitting between the two qubit states, as well as the energy of higher (orbital) excited states. Furthermore, the QPC can be used to monitor the inter-dot tunnel barrier, both qualitatively (from the curvature of lines in the honeycomb diagram) and quantitatively (by performing photon-assisted tunneling spectroscopy to measure the splitting between the one-electron bonding and anti-bonding state [16]). In principle, it is even possible to use the lock-in technique to measure the exchange splitting J between the delocalized two-electron singlet and triplet spin states.

We can thus determine all relevant parameters of the two-spin system without performing transport measurements. The essential advantage of the QPC technique is that it works even for a dot that is very weakly coupled to just a *single* reservoir, with a tunnel rate between zero and ~100 kHz (limited by the bandwidth of the current measurement setup). This gives us more freedom to design simpler dots with fewer gates, which could therefore be easier to operate.

3 Read-out

3.1 Spin-to-charge conversion

The magnetic moment associated with the electron spin is very small (equal to the Bohr magneton μ_B) and therefore hard to measure directly. However, by correlating the spin states to different charge states and subsequently measuring the charge on the dot, the spin state can be determined [1]. This way, measurement of a single spin is replaced by measurement of a single charge, which is a much easier task. The remaining challenge is to find a reliable method for correlating the spin states to different charge states. We have experimentally demonstrated two methods for such a spin-to-charge conversion in a single quantum dot. They are both outlined in Fig. 2.

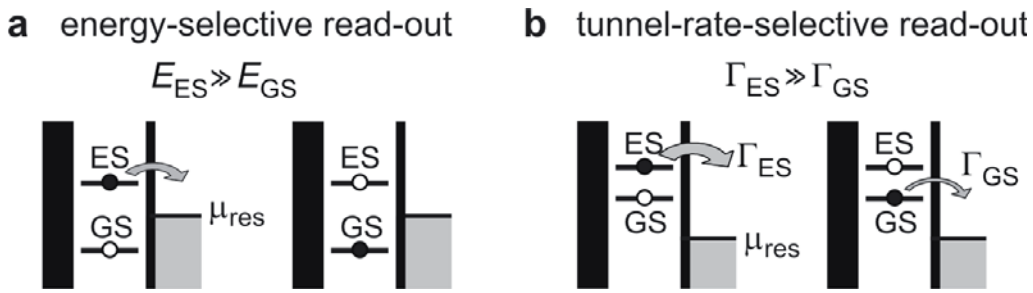

Fig. 2 Schematic energy diagrams depicting spin-to-charge conversion based on a difference in *energy* (a) between two states, or on a difference in *tunnel rate* (b).

In one method, a difference in *energy* between the spin states is used for spin-to-charge conversion. In this energy-selective readout (E-RO), the energy levels are positioned around the electrochemical potential of the reservoir μ_{res} as depicted in Fig. 2a, such that one electron can tunnel off the dot from the spin excited state (ES), whereas tunneling from the ground state (GS), is energetically forbidden. Therefore, if the charge measurement reveals that one electron tunnels off the dot, the state was ES, while if no electron tunnels off the dot, the state was GS. (A conceptually similar scheme has also allowed single-shot readout of a superconducting charge qubit [17]).

Alternatively, spin-to-charge conversion can be achieved by exploiting a difference in *tunnel rates* of the different spin states to the reservoir. The concept of this tunnel-rate-selective readout (TR-RO) is outlined in Fig. 2b, for the case that the tunnel rate from ES to the reservoir, Γ_{ES}, is much higher than the tunnel rate from GS, Γ_{GS}, i.e. $\Gamma_{ES} \gg \Gamma_{GS}$. Then, the spin state can be read out as follows. At time $t = 0$, the levels of both ES and GS are positioned far above μ_{res}, so that one electron is energetically allowed to tunnel off the dot regardless of the spin state. Then, at a time $t = \tau$, where $\Gamma_{GS}^{-1} \gg \tau \gg \Gamma_{ES}^{-1}$, an electron will have tunneled off the dot with a very high probability if the state was ES, but most likely no tunneling will have occurred if the state was GS. Thus, the spin information is converted to charge information, and a measurement of the number of electrons on the dot reveals the original spin state. We note that both methods presented here can in principle also be used to read out the orbital state of the quantum dot.

In the experiments, one of the two tunnel barriers defining a single quantum dot is completely pinched off, so that the dot is only coupled to one reservoir. The "plunger" gate (P) is used to apply fast voltage pulses to the device, with a typical pulse rise time of about 1 ns. The conductance of the QPC is tuned to about e^2/h, making it very sensitive to the number of electrons on the dot. A voltage bias of about 0.8 mV induces a current through the QPC of about 30 nA. The number of electrons on the dot is then determined from pulse spectroscopy measurements [15]. All experiments are performed in a dilution refrigerator at $T = 20$ mK, in the presence of an in-plane magnetic field up to 14 T.

3.2 Single-shot read-out of a single electron spin

We first discuss the demonstration of single-shot readout of a single electron spin using the E-RO technique [4]. A quantum dot containing zero or one electron is tunnel coupled to a single reservoir and electrostatically coupled to a QPC that serves as an electrometer. By operating the electrometer at a bandwidth of 40 kHz, the number of electrons on the dot can be determined in about 10 μs.

To test the single-spin measurement technique, we use an experimental procedure based on three stages: 1) empty the dot, 2) inject one electron with unknown spin, and 3) measure its spin state. The different stages are controlled by voltage pulses on a gate electrode as in Fig. 3a, which shift the dot energy levels as shown in Fig. 3c. Before the pulse the dot is empty, as both the spin-up and spin-down levels are above the electrochemical potential of the reservoir μ_{res}. Then a voltage pulse pulls both levels below μ_{res}. It is now energetically allowed for an electron to tunnel onto the dot, which will happen after a typical time $\sim 1/\Gamma$. The particular electron can have spin-up or spin-down, shown in the lower and upper

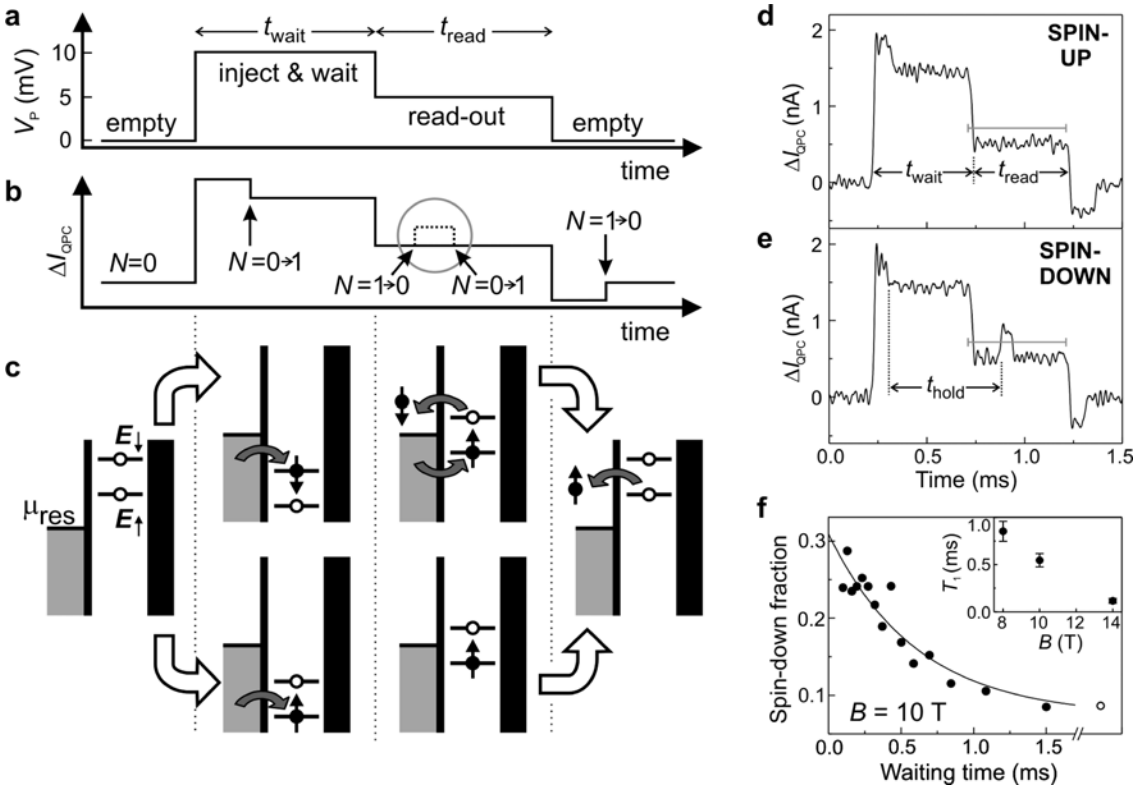

Fig. 3 Energy-selective read-out of a single electron spin. (a) Two-level voltage pulse scheme. (b) Expected response of ΔI_{QPC} to the voltage pulses. (c) Energy diagrams depicting the levels during the different stages of the pulse. (d) Measurement outcome corresponding to a spin-up electron. (e) Idem for a spin-down electron. (f) Dependence of the fraction of spin-down electrons on the waiting time, showing a clear exponential decay. The open circle results from a measurement where the pulse shape is modified, such that only spin-up electrons are injected. Inset: the spin relaxation time T_1 as a function of the in-plane magnetic field $B_{||}$.

diagram respectively. During this stage of the pulse, lasting t_{wait}, the electron is trapped on the dot and Coulomb blockade prevents a second electron to be added. After t_{wait}, the pulse is reduced, in order to position the energy levels in the readout configuration. If the electron has spin-up, its energy level is below μ_{res}, so the electron remains on the dot. If the electron has spin-down, its energy level is above μ_{res}, so the electron tunnels to the reservoir after a typical time $\sim 1/\Gamma_\downarrow$. Now Coulomb blockade is lifted and an electron with spin-up can tunnel onto the dot. This occurs on a timescale $\sim 1/\Gamma_\uparrow$. After t_{read}, the pulse ends and the dot is emptied again.

The expected QPC-response, ΔI_{QPC}, to such a two-level pulse is the sum of two contributions (Fig. 3b). First, due to a capacitive coupling between pulse-gate and QPC, ΔI_{QPC} will change proportionally to the pulse amplitude. Thus, ΔI_{QPC} versus time resembles a two-level pulse. Second, ΔI_{QPC} tracks the charge on the dot, i.e. it goes up whenever an electron tunnels off the dot, and it goes down by the same amount when an electron tunnels onto the dot. Therefore, if the dot contains a spin-down electron at the start of the readout stage, ΔI_{QPC} should go up and then down again. We thus expect a characteristic step in ΔI_{QPC} during t_{read} for a spin-down electron (dotted trace inside grey circle). In contrast, ΔI_{QPC} should be flat during t_{read} for a spin-up electron. Measuring whether a step is present or absent during the readout stage constitutes the spin measurement.

Figure 3d and e show experimental traces of the pulse response at an in-plane magnetic field B of 10 T, where the Zeeman splitting ΔE_Z is ~200 μeV. We emphasize that each trace involves injecting one

particular electron on the dot and subsequently measuring its spin state. Each trace is therefore a single-shot measurement. The experimentally obtained traces fall into two different classes; most traces qualitatively resemble the one in Fig. 3d, some resemble the one in Fig. 3e (and sometimes no electron was injected during the injection stage; such cases are detected and ignored). These two typical traces indeed correspond to the signals expected for a spin-up and a spin-down electron (Fig. 3b), a strong indication that the electron in Fig. 3d was spin-up and in Fig. 3e spin-down. The distinct signature of the two types of responses in ΔI_{QPC} permits a simple criterion for identifying the spin: if ΔI_{QPC} crosses the threshold value (grey line in Fig. 3d and e), the electron is declared 'spin-down'; otherwise it is declared 'spin-up'.

In order to further establish the correspondence between the actual spin state and the outcome of the spin measurement, the probability to have a spin-down at the beginning of the readout stage is changed, and compared with the fraction of traces in which the electron is declared 'spin-down'. As t_{wait} is increased, the time between injection and readout, t_{hold}, will vary accordingly ($t_{hold} \sim t_{wait}$). The probability for the spin to be down at the start of t_{read} will thus decay exponentially to zero, since electrons in the excited spin state will relax to the ground state ($kT \ll \Delta E_Z$). The fact that the expected exponential decay is clearly reflected in the data (see Fig. 3f) confirms the validity of the spin readout procedure. A detailed analysis reveals that the visibility of the single-shot measurement is ~65%.

The spin relaxation time T_1 is plotted as a function of the in-plane magnetic field B in the inset of Fig. 3f. We find that T_1 increases with decreasing B, reaching 0.85 ms at 8 T. For smaller field the Zeeman energy was too small to perform reliable readout measurements. Both the magnitude and the magnetic field dependence of T_1 are consistent with spin–orbit induced decay where the excess energy is released into the phonon bath [18].

The E-RO has made the first all-electrical single-shot readout of a single electron spin possible. However, there are a couple of drawbacks to this method: (i) E-RO requires an energy splitting of the spin states larger than the thermal energy of the electrons in the reservoir. Thus, for a single spin the readout is only effective at very low electron temperature and high magnetic fields (8 T and higher in Ref. [4]). Also, interesting effects occurring close to degeneracy, e.g. near the singlet-triplet crossing for two electrons, cannot be probed. (ii) Since the E-RO relies on precise positioning of the spin levels with respect to the reservoir, it is very sensitive to fluctuations in the electrostatic potential. Background charge fluctuations [19], active even in today's most stable devices, can easily push the levels out of the readout configuration. (iii) High-frequency noise can spoil the E-RO by inducing photon-assisted tunneling from the spin ground state to the reservoir. Since the QPC is a source of shot noise, this limits the current through the QPC and thereby the bandwidth of the charge detection [20]. These constraints have fueled the search for a better method for spin-to-charge conversion, and have led to the demonstration of the tunnel-rate-selective readout (TR-RO) [5], which we treat in the next section.

3.3 Single-shot read-out of two-electron spin states

The main ingredient necessary for TR-RO is a spin dependence of the tunnel rates. For a single electron, this spin dependence can be obtained in the Quantum Hall regime, where a high spin-selectivity is induced by the spatial separation of spin-resolved edge channels [2, 21]. TR-RO can also be used for readout of the spin states of a two-electron dot, where the electrons are either in the spin-singlet ground state, denoted by $|S\rangle$, or in a spin-triplet state, denoted by $|T\rangle$. In $|S\rangle$, the two electrons both occupy the lowest orbital, but in $|T\rangle$ one electron is in the first excited orbital. Since the wave function in this excited orbital has more weight near the edge of the dot [22], the coupling to the reservoir is stronger than for the lowest orbital. Therefore, the tunnel rate from a triplet state to the reservoir Γ_T is much larger than the rate from the singlet state Γ_S, i.e. $\Gamma_T \gg \Gamma_S$ [23]. This spin dependence is used to experimentally demonstrate the TR-RO for two electrons.

We tune the dot to the $N = 1 \leftrightarrow 2$ transition in a small in-plane magnetic field $B_{||}$ of 0.02 T. Here, the energy difference between $|T\rangle$ and the ground state $|S\rangle$, E_{ST}, is about 1 meV. From measurements of the tunnel rates [15], we estimate the ratio Γ_T/Γ_S to be on the order of 20. A similar ratio was found previously in transport measurements on a different device [23]. This permits a readout visibility larger than

80%. We implement the TR-RO by applying voltage pulses as depicted in Fig. 4a to the plunger gate. Figure 4b shows the expected response of I_{QPC} to the pulse, and Fig. 4c gives the level diagrams in the three different stages.

Before the pulse starts, there is one electron on the dot. Then, the pulse pulls the levels down so that a second electron can tunnel onto the dot ($N = 1 \rightarrow 2$), forming either a singlet or a triplet state with the first electron. The probability that a triplet state is formed is given by $3\Gamma_T/(\Gamma_S + 3\Gamma_T)$, where the factor of 3 is due to the degeneracy of the triplets. After a variable waiting time t_{wait}, the pulse ends and the readout process is initiated, during which one electron can leave the dot again. The rate for tunneling off depends on the two-electron state, resulting in the desired spin-to-charge conversion. The QPC is used to detect the number of electrons on the dot. Due to the direct capacitive coupling of the plunger gate to the QPC channel, ΔI_{QPC} follows the pulse shape. Tunneling of an electron on or off the dot gives an additional step in ΔI_{QPC} [4, 20, 24], as indicated by the arrows in Fig. 4b.

We tune Γ_S to 2.5 kHz, and therefore $\Gamma_T \sim 50$ kHz. In order to achieve a good signal-to-noise ratio in I_{QPC}, the signal is sent through an external 20 kHz low-pass filter. As a result, many of the tunnel events from $|T\rangle$ will not be resolved, but the tunneling from $|S\rangle$ should be clearly visible. Figure 4d shows several traces of ΔI_{QPC}, from the last part (300 μs) of the pulse to the end of the readout stage (see inset), for a waiting time of 0.8 ms. In some traces, there are clear steps in ΔI_{QPC}, due to an electron tunneling off the dot. In other traces, the tunneling occurs faster than the filter bandwidth. In order to discriminate between $|S\rangle$ and $|T\rangle$, we first choose a readout time τ (indicated by a vertical dashed line in Fig. 4d) and measure the number of electrons on the dot at that time by comparing ΔI_{QPC} to a threshold value (as indicated by the horizontal dashed line in the bottom trace of Fig. 4d). If ΔI_{QPC} is below the threshold, it means $N = 2$ and we declare the state 'S'. If ΔI_{QPC} is above the threshold, it follows that $N = 1$ and the state is declared 'T'.

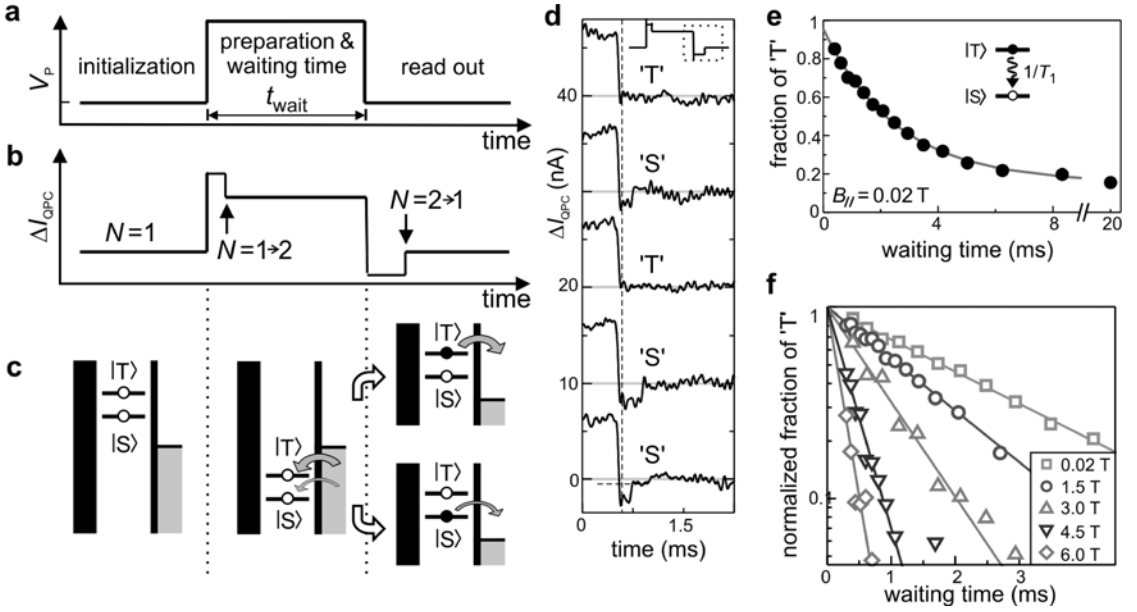

Fig. 4 Single-shot readout of two-electron spin states. (a) Voltage pulse waveform applied to one of the gate electrodes. (b) Response of the QPC-current to the waveform of (a). (c) Energy diagrams indicating the positions of the levels during the three stages. In the final stage, spin is converted to charge information due to the difference in tunnel rates for states $|S\rangle$ and $|T\rangle$. (d) Real-time traces of ΔI_{QPC} during the last part of the waveform (dashed box in the inset), for $t_{wait} = 0.8$ ms. At the vertical dashed line, N is determined by comparison with a threshold (horizontal dashed line in bottom trace) and the spin state is declared 'T' or 'S' accordingly. (e) Fraction of 'T' as a function of waiting time at $B_{\|} = 0.02$ T, showing a single-exponential decay with a time constant T_1 of 2.58 ms. (f) Normalized fraction of 'T' versus t_{wait} for different values of $B_{\|}$.

To verify that 'T' and 'S' indeed correspond to the spin states $|\mathrm{T}\rangle$ and $|\mathrm{S}\rangle$, we change the relative occupation probabilities by varying the waiting time. The probability that the electrons are in $|\mathrm{T}\rangle$, P_T, decays exponentially with the waiting time. Therefore, as we make the waiting time longer, we should observe an exponential decay of the fraction of traces that are declared 'T'. We take 625 traces similar to those in Fig. 4d for each of 15 different waiting times. Note that the two-electron state is formed on a timescale (of order $1/\Gamma_\mathrm{T}$) much shorter than the shortest t_wait used (400 μs). In Fig. 4e, we plot the fraction of traces declared 'T' as a function of t_wait. We see that this fraction decays exponentially, showing that we can indeed read out the two-electron spin states. The single-shot measurement visibility is found to be 81%. A fit to the data yields a triplet-to-singlet relaxation time $T_1 = (2.58 \pm 0.09)$ ms, which is more than an order of magnitude longer than the lower bound found in Ref. [25].

We further study the relaxation between triplet and singlet states by repeating the measurement of Fig. 4e at different values of the in-plane magnetic field $B_\parallel$. Figure 4f shows the decay of the fraction of 'T', normalized to the fraction of 'T' $t_\mathrm{wait} = 0$, on a logarithmic scale. The data follow a single-exponential decay at all fields. The dominant relaxation mechanisms for large values of E_ST are believed to originate from the spin–orbit interaction [18]. A second-order polynomial fit to the data yields $1/T_1$ [kHz] $= (0.39 \pm 0.03) + (0.10 \pm 0.02) \cdot B_\parallel^2$ [T], with a negligible linear term.

The TR-RO method shown above is very suitable to distinguish the single-dot singlet from the triplet states, as these have a large difference in tunnel rates due to their different orbital wavefunctions. However, for quantum information processing, the two-level system formed by the spin-up and spin-down state of a single electron is more relevant. TR-RO can in principle also be used for read-out of these two states, provided they have a significant difference in tunnel rates. This can be achieved by applying a large perpendicular magnetic field, i.e. in the quantum Hall regime. In this case, the reservoir can exhibit spin-resolved edge channels that are spatially separated, leading to an effective difference in the tunnel barrier seen by spin-up and spin-down [2, 21]. To reduce the magnetic field required to reach a certain spin selectivity, large gates next to the quantum dot could be used to locally reduce the electron density in the reservoirs [26]. Then the reservoir could be strongly spin-polarized, leading to a large spin-selectivity, while the electron in the dot would experience only a moderate magnetic field.

4 Initialization

We have demonstrated initialization [4] of the spin to the pure state ↑ – the desired initial state for most quantum algorithms. By waiting long enough, energy relaxation will cause the spin on the dot to relax to the ↑ ground state (Fig. 5a). This is a very simple and robust initialization approach, which can be used for any magnetic field orientation (provided that $g\mu_\mathrm{B}B > 5\,k_\mathrm{B}T$). However, as it takes about 5 T_1 to reach equilibrium, it is also a very slow procedure, especially at lower magnetic fields, where the spin relaxation time T_1 might be very long.

A faster initialization method is to place the dot in the read-out configuration (Fig. 5b), where a spin-up electron will stay on the dot, whereas a spin-down electron will be replaced by a spin-up [4]. After

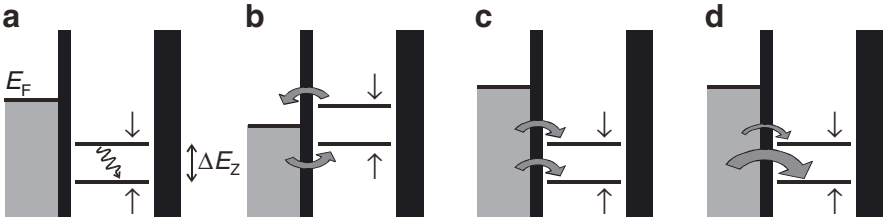

Fig. 5 Schematic energy diagrams depicting initialization procedures in a large parallel or perpendicular magnetic field. (a) Spin relaxation to pure state ↑. (b) The 'read-out' configuration can result in ↑ faster. (c) Random spin injection gives a statistical mixture of ↑ and ↓. (d) In a large perpendicular field providing a strong spin-selectivity, injection results mostly in ↑.

waiting a few times the sum of the typical tunnel times for spin-up and spin-down ($\sim 1/\Gamma_\uparrow + 1/\Gamma_\downarrow$), the spin will have a large probability to be in the $\uparrow$ state. This initialization procedure can therefore be quite fast (<1 ms), depending on the tunnel rates.

We also have the possibility to initialize the dot to a mixed state, where the spin is probabilistically in $\uparrow$ or $\downarrow$. In Ref. [4], mixed-state initialization was demonstrated in a parallel field by first emptying the dot, followed by placing both spin levels below E_F during the 'injection stage' (Fig. 5c). The dot is then randomly filled with either a spin-up or a spin-down electron. This can be very useful, e.g. to test two-spin operations.

In a large perpendicular field providing a strong spin-selectivity, initialization to the $\uparrow$ state is possible via spin relaxation (Fig. 5a) or via direct injection (Fig. 5d). Initialization to a mixed state (or in fact to any state other than $\downarrow$) is very difficult due to the spin-selectivity. It probably requires the ability to coherently rotate the spin from $\uparrow$ to $\downarrow$ (see Section 6).

5 Relaxation and decoherence times

The long-term potential of GaAs quantum dots as electron spin qubits clearly depends crucially on the spin relaxation and decoherence times, T_1 and T_2 respectively. We have shown that the single-spin relaxation time, T_1, can be very long – on the order of 1 ms at 8 Tesla [4, 5]. The dominant relaxation mechanism at large magnetic field is the coupling of the electron spin to phonons, mediated by the spin–orbit interaction [18]. Below about 100 mT, spin relaxation is dominated by hyperfine interaction with the nuclear spins in the host material [7].

The fundamental quantity of interest for spin qubits is the decoherence time of a single electron spin in a quantum dot, T_2. Experiments have shown that the (time-ensemble averaged) spin dephasing time T_2^* is about 10 ns, limited by hyperfine interactions with the fluctuating nuclear spin ensemble [7–9]. Using spin-echo techniques, a decoherence time T_2 exceeding a microsecond [9] was demonstrated.

6 Coherent single-spin manipulation: ESR

The key requirement for an actual spin qubit is the ability to coherently manipulate the spin states. This milestone has recently been achieved [9, 10]. To create controllable superpositions of $\uparrow$ and $\downarrow$, the well-known electron spin resonance (ESR) effect can be used. A microwave magnetic field B_{ac} oscillating in the plane perpendicular to B, at a frequency $f = g\mu_B B/h$ (in resonance with the spin precession about B) causes the spin to make transitions between $\uparrow$ and $\downarrow$. Properly timed bursts of microwave power tip the spin state over a controlled angle, e.g. 90° or 180°. For a Rabi period of 150 ns, we need a microwave field strength B_{ac} of ~1 mT.

The oscillating magnetic field is generated by sending an alternating current through an on-chip wire running close by the dot (Fig. 6a). If the wire is placed well within one wavelength from the quantum dot (which is about 30 cm at 1 GHz near the surface of a GaAs substrate), the dot is in the near-field region and the electric and magnetic field distribution produced by the AC current should be the same as for a DC current. With a wire 200 nm from the dot, a current of ~1 mA should thus generate a magnetic field of about 1 mT and no electric field at the position of the dot. To minimize reflection and radiation losses, the wire is designed to be a shorted coplanar stripline (Fig. 6c) with a 50 Ω impedance. To reduce dissipative losses, the wire could be made from a superconducting material.

To detect the electron spin resonance (ESR), various methods have been proposed, either using transport measurements [27] or relying on charge detection [28]. In both cases, the required spin-to-charge conversion is achieved by positioning the dot levels around the Fermi energy of the reservoir. The ESR-field induces spin flips, exciting $\uparrow$ electrons to $\downarrow$, which can then tunnel out of the dot. This leads to an average current [27] or to a change in the average occupation of the dot [28]. However, in this configuration the dot is particularly sensitive to spurious effects induced by the microwaves, such as $\uparrow$ electrons being excited out of the dot via thermal excitation or photon-assisted tunneling. These processes can completely obscure the spin resonance. A more convenient way to detect ESR is therefore to use a dou-

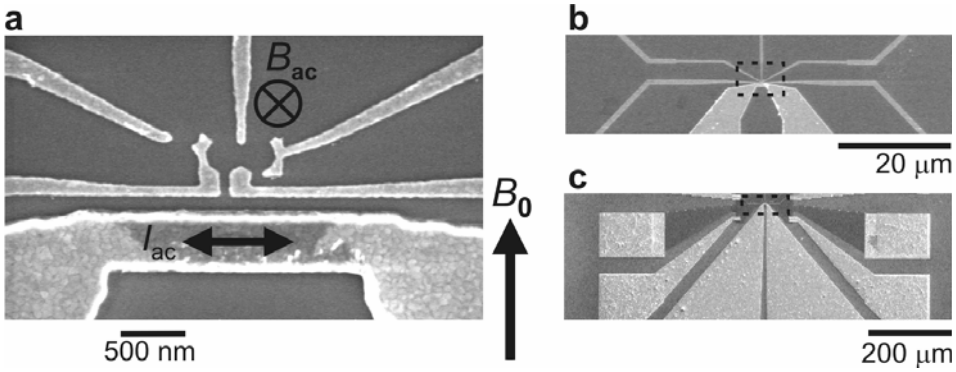

Fig. 6 On-chip wire to apply microwaves to a nearby quantum dot. (a) Scanning electron microscope image of a device consisting of a double quantum dot in close proximity to a metal wire. An AC current through the wire, I_{ac}, generates an oscillating magnetic field, B_{ac}, perpendicular to the plane. If the AC frequency is resonant with the Zeeman splitting due to a large static in-plane magnetic field, B, a spin on the dot will rotate. (b) and (c) Large-scale views of the wire, designed to be a 50 Ω coplanar stripline.

ble dot in the Pauli blockade regime [10]. In this case, the detection of spin resonance can be achieved by measuring the current resulting from mixing of singlet and triplet states. This mixing is enhanced if an electron spin can be flipped by the ESR field, resulting in an enhanced current through the device.

7 Coherent spin interactions: $\sqrt{\text{SWAP}}$

Two electron spins S_1 and S_2 in neighbouring quantum dots are coupled to each other by the exchange interaction, which takes the form $J(t) = S_1 \cdot S_2$. If the double dot is filled with two identical spins, the interaction does not change their orientation. However, if the left electron spin starts out being ↑ and the right one ↓, then the states of the two spins will be swapped after a certain time. An interaction active for half this time performs the $\sqrt{\text{SWAP}}$ gate, which has been shown to be universal for quantum computation when combined with single qubit rotations [29]. In fact, the exchange interaction is even universal by itself when the state of each qubit is encoded in the state of three electron spins [30].

The strength $J(t)$ of the exchange interaction depends on the overlap of the two electron wavefunctions, which varies exponentially with the voltage applied to the gate controlling the inter-dot tunnel barrier. By applying a (positive) voltage pulse with a certain amplitude and duration, the exchange interaction can be temporarily turned on, thereby performing a $\sqrt{\text{SWAP}}$ gate [1]. Such coherent manipulation of coupled spin states has recently been achieved [9].

8 Conclusion

We have argued that single electrons trapped in GaAs lateral quantum dots are promising candidates for implementing a spin qubit. The 'hardware' for such a system has been realized: a device consisting of two coupled quantum dots that can be filled with one electron spin each, flanked by two quantum point contacts. Using these QPCs as charge detectors, all relevant parameters of the double dot can be determined. In addition, we have developed a technique to measure the spin orientation of an *individual* electron. Recently, the ability to generate strong microwave magnetic fields close to the dot has been used to demonstrate driven coherent oscillations of a single electron spin [10]. In combination with coherent manipulation of coupled spins [9], these achievements could be used in the future to create a universal quantum gate.

Acknowledgements We thank C.J.P.M. Harmans, W.G. van der Wiel, M. Blaauboer, S. Tarucha, and D. Loss for useful discussions. We acknowledge financial support from the Specially Promoted Research Grant-in-Aid for Sci-

entific Research from the Japanese Ministry of Science; DARPA grant DAAD19-01-1-0659 of the QuIST program; the Dutch Organization for Fundamental Research on Matter (FOM); and the European Union through a TMR Program Network.

References

[1] D. Loss and D. P. DiVincenzo, Phys. Rev. A **57**, 120 (1998).
[2] M. Ciorga et al., Phys. Rev. B **61**, 16315 (2000).
[3] J. M. Elzerman et al., Phys. Rev. B **67**, 161308 (2003).
[4] J. M. Elzerman et al., Nature **430**, 431 (2004).
[5] R. Hanson et al., Phys. Rev. Lett. **94**, 196802 (2005).
[6] K. Ono, D. G. Austing, Y. Tokura, and S. Tarucha, Science **297**, 1313 (2002).
[7] A. C. Johnson et al., Nature **435**, 925 (2005).
[8] F. H. L. Koppens, J. A. Folk et al., Science **309**, 1346 (2005).
[9] J. R. Petta et al., Science **309**, 2180 (2005).
[10] F. H. L. Koppens et al., Nature (in print).
[11] D. P. DiVincenzo, Fortschr. Phys. **48**, 771 (2000).
[12] R. M. Potok et al., Phys. Rev. Lett. **91**, 016802 (2003).
[13] R. Hanson et al., Phys. Rev. Lett. **91**, 196802 (2003).
[14] M. Field et al., Phys. Rev. Lett. **70**, 1311 (1993).
[15] J. M. Elzerman et al., Appl. Phys. Lett. **84**, 4617 (2004).
[16] J. R. Petta et al., Phys. Rev. Lett. **93**, 186802 (2004).
[17] O. Astafiev et al., Phys. Rev. B **69**, 180507 (2004).
[18] V. N. Golovach, A. Khaetskii, and D. Loss, Phys. Rev. Lett. **93**, 016601 (2004).
[19] S. W. Jung, T. Fujisawa, Y. Hirayama, and Y. H. Jeong, Appl. Phys. Lett. **85**, 768 (2004).
[20] L. M. K. Vandersypen et al., Appl. Phys. Lett. **85**, 4394 (2004).
[21] M. Ciorga et al., Appl. Phys. Lett. **80**, 2177 (2002).
[22] L. P. Kouwenhoven, D. G. Austing, and S. Tarucha, Rep. Prog. Phys. **64**, 701 (2001).
[23] R. Hanson et al., Proceedings of the 39th Rencontres de Moriond, see also cond-mat/0407793.
[24] R. Schleser et al., Appl. Phys. Lett. **85**, 2005 (2004).
[25] T. Fujisawa, D. G. Austing, Y. Tokura, Y. Hirayama, and S. Tarucha, Nature **419**, 278 (2002).
[26] L. M. K. Vandersypen et al., quant-ph/0207059.
[27] H. A. Engel and D. Loss, Phys. Rev. Lett. **86**, 4648 (2001).
[28] I. Martin, D. Mozyrsky, and H. W. Jiang, Phys. Rev. Lett. **90**, 018301 (2003).
[29] G. Burkard, D. Loss, and D. P. DiVincenzo, Phys. Rev. B **59**, 2070 (1999).
[30] D. P. DiVincenzo, D. P. Bacon, D. A. Lidar, and K. B. Whaley, Nature **408**, 339 (2000).

